THE ARCHIVE OF MECHANICAL ENGINEERING

Vol. LI 2004 Number 2

Key words: *modelling, dynamics, offshore crane*

*MAREK OSINSKI**), *ANDRZEJ MACZYŃSKI***), *STANISLAW WOJCIECH****)

THE INFLUENCE OF SHIP'S MOTION IN REGULAR WAVE ON DYNAMICS OF AN OFFSHORE CRANE

The paper presents the numerical model of a supply vessel–load–crane–offshore vessel system for simulation of heave motion and dynamic analysis of the system during critical phases of the handling operation: taking the load off from and lowering it to a moving base. The model enables extreme forces in elements and deflection of the structure to be determined. Different operating and emergency conditions can be simulated (e.g. horizontal motion of a supply vessel). The elaborated software can be applied also for determination of derated load charts and ultimate crane capacity (sequence of failure).

1. Introduction

Offshore cranes are handling facilities permanently mounted on offshore installations (platform, drilling rig, production vessel etc.) and primarily intended for material handling from and to the deck of a supply vessel. The cranes are subjected to a variety of hazards which normally do not exist for any standard onshore cranes. The most important cause of hazards is operation in the open sea in a harsh environment (wind and wave motion). Such an environment creates operational challenges for the crane driver and for the hook men. These operational difficulties induce additional vertical and horizontal (side- and off-lead) dynamic loads. All these loads are difficult to

*) *TTS-Aktro AS, Hjelest, Norway; E-mail: marek.osinski@natoil.com*

**) *Faculty of Mechanical Engineering and Information Sciences, University of Belsko-Biała; Willowa 2, 43-309 Bielsko-Biala, Poland; E-mail: amaczynski@th.bielsko.pl*

***) *Faculty of Mechanical Engineering and Information Sciences, University of Belsko-Biała; Willowa 2, 43-309 Bielsko-Biala, Poland; E-mail: swojciech@th.bielsko.pl*

predict and quantify. It is also very important that such loading conditions can not be easily simulated on the crane test stand.

When designing an offshore crane, a very important part of calculation is determination of the dynamic coefficient. According to crane standards, this coefficient can be evaluated by the normally used simplified method or by a full motion response analysis. The simplified method is based on the crane's total stiffness and adopts the energy balance equation of the system. The motion response analysis investigates the motion behaviour of the offshore installation, the offshore crane, supply vessel and all other elements of the system such as lifted load, shock absorber or motion compensator (if any).

The literature concerned with modelling of offshore cranes is quite large. According to the problem considered authors use 2D models [1], [2], [3], [4], [5] or 3D models [6], [7] with a different number of degrees of freedom. In some papers, e.g. in [1] and [8] it is assumed that the deck of a vessel moves only in a vertical direction (heave) harmonically with known amplitude, frequency and phase. Motion of a ship in two directions is investigated in [2], where two kinds of input are considered: – harmonic and periodic (a sum of three harmonic components). In [9] hydrodynamic forces influence the ship motion. In the case of regular waves, hydrodynamic forces can be treated as a sum of principal and diffraction part of forces. This model is in agreement with the theory of wave motion presented in [10]. Excitation forces acting in directions of three generalized coordinates (two linear displacements and one rotation) are defined in [4] and [5]. These forces can be divided into a periodically changing component and the constant drift forces. Additionally, the hydrodynamic forces are taken into consideration. In [7], a ship with a modelled crane is swaying, surging, heaving, pitching and rolling. The sway, surge and heave motions are measured for the reference point. In paper [6] the ADAMS package is used to analyse dynamics of a vessel. The sea is modelled as a massless part able to slide vertically with respect to the ground. Its motion can be defined in two ways: by a spline function of time based on an external data file derived from real sea trials of the actual crane, or by an analytic function defined using a pseudostochastic model of wave elevation. The problem of minimization of load slewing for offshore cranes is discussed e.g. in [1], [2], [7], [11]; whereas control of the hoisting drum motion is the main subject of [6], [12] and [13].

Establishing a reliable model taking into account all important factors and dynamic relations between elements of the supply vessel–load–crane–offshore vessel system was the objective of the presented analysis. The planar model of such a system was elaborated to analyse the forces acting in joints, ropes and hydraulic cylinders, and for motion analysis of the system

during the two most critical phases of the reloading operation: lifting the load from or lowering it to the deck of a supply vessel. The model includes flexibility of the hoist rope, jib, pedestal adapter, luff system, characteristics of the shock absorber.

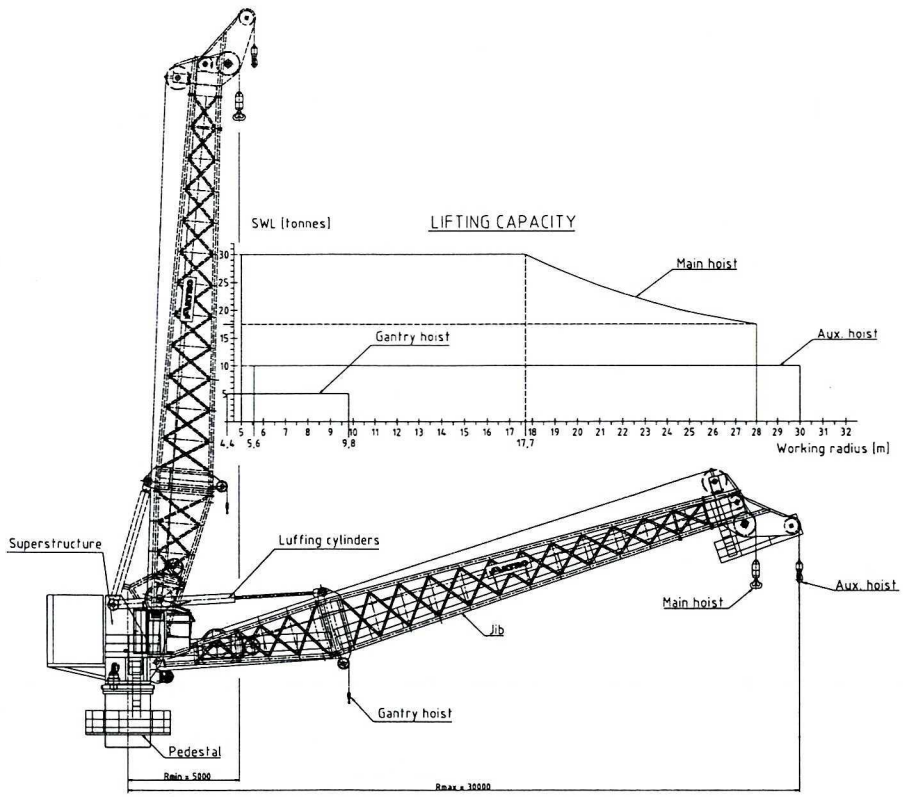

Fig. 1. TTS-AKTRO off-shore crane

The model has been developed for cranes designed and manufactured by the company TTS-AKTRO A.S., Norway. Numerical calculations have been performed for the SWL 30T pedestal crane, presented in Figure 1. The crane was installed on the pipe-laying vessel Kommandor 3000.

The results of some numerical calculations are also included in this paper.

2. Discretization of the system

The paper presents the planar model of an offshore crane installed on a offshore vessel, lifting a load from or lowering it to the deck of a supply vessel.

In order to formulate equations of motion, the system was divided into the following subsystems:

{1} the off-shore vessel with the crane pedestal and slewing platform,
{2} jib,
{3} hydraulic cylinder,
{4} shock absorber,
{5} hoisting winch with wire rope,
{6} load.

The analysed system is a complex one and consists of elements with various properties. Among them the following can be indicated:

- elements with continuous distribution of mass and stiffness
  - with bending and torsional flexibility (jib),
  - with longitudinal flexibility (hydraulic cylinder),
- rigid elements of considerable mass (load, slewing platform),
- massless flexible elements (ropes).

The system and the defined subsystems are shown in Figure 2.

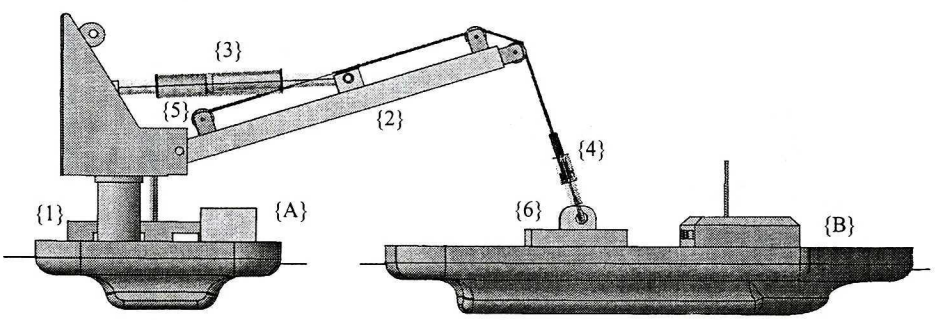

Fig. 2. Offshore vessel – load – supply vessel system

One of the methods that can be used to digitise a subsystem with continuous distribution of mass and stiffness is the rigid finite element method (RFEM), [14] and [15]. According to this method, the flexible member is divided into a number of rigid mass elements, connected by massless, spring-damping elements. The method has been developed on at the Technical University of Gdańsk (Kruszewski, Wittbrodt), at the Technical University of Szczecin (Marchelek), and at the Technical University of Łódź (Wojciech). It has been largely used in the dynamics of machines, including cranes [16], [17] and manipulators [18], [19]. It is especially useful in analysis of systems with changing configuration, for which large movements of the base of flexible elements are combined with the vibrations of the elements [18]. The method of rigid finite elements does not compete with the finite

element method (FEM) [20]. Thanks to its simplicity, it complements the FEM systems pack (ANSYS, NASTRAN, NISA etc.) wherever the usage of FEM is difficult or not worth while. The idea of this method is presented in the following chapters of this paper.

It is assumed that the movement of $\{A\}$ – offshore vessel and $\{B\}$ – supply vessel are known and, thus these coordinates and their derivatives are also know:

$$\{x_A = x_A(t),\ y_A = y_A(t),\ \varphi_A = \varphi_A(t) \tag{1}$$

and:

$$\{x_B = x_B(t),\ y_B = y_B(t),\ \varphi_B = \varphi_B(t) \tag{2}$$

3. Discretization of elements with continuous distribution of mass andflexibility

The elements with continuous distribution of mass and flexibility are:

- Subsystems {1} and {2}, which may be treated as beams with variable cross sectional properties, longitudinal and bending flexibility,
- Subsystems {3} and {4}, which are also elements with continuous distribution of mass but longitudinal flexibility only.

The discrete models of both types of elements (with a beam and with a hydraulic cylinder), obtained by using the finite rigid element method, are presented below.

3.1. Model of a beam with longitudinal and bending flexibility

Figure 3 shows the beam and its model, obtained using the rigid finite element method. The beam has been divided into $n_k + 1$ rigid elements (rfe) and n_k dimensionless and massless spring – damping elements (sde). The methods of division and of determining the parameters of rfe and sde have been presented in work [15], both for beams of constant and variable cross-sectional parameters.

The movement of the system is characterised by $3(n_k + 1)$ parameters, which are the components of the vector:

$$q^{(k)} = \left[q_0^{(k)}\ q_1^{(k)} \ldots q_i^{(k)} \ldots q_{n_k}^{(k)} \right]^T \tag{3}$$

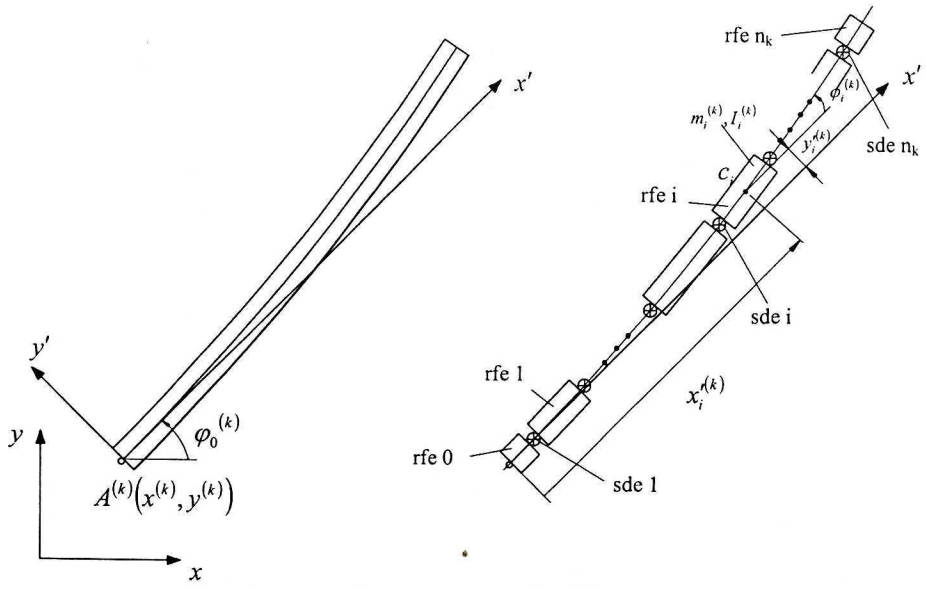

Fig. 3. Discretization of flexible beam

where:

$q_0^{(k)} = \left[x_A^{(k)}\ y_A^{(k)}\ \varphi_0^{(k)}\right]^T$ – is the vector of coordinates of the system describing the position of element 0 (the base motion),

$q_i^{(k)} = \left[x_i'^{(k)}\ y_i'^{(k)}\ \varphi_i'^{(k)}\right]^T$ – is the vector describing the position of the i-th rigid element in relation to element number 0. $i = 1,...,n_k$ (Figure 4).

The meaning of the components of vector $q_i^{(k)}$ is as follows:

x_i' – corresponds to longitudinal deformation,

y_i' – corresponds to shearing,

φ_i' – corresponds to bending.

According to Figure 4, the coordinates of any point D of the i-th element are given by the formulae:

$$\begin{cases} x_D^{(k)} = x_A^{(k)} + x_D'^{(k)} \cos\varphi_0^{(k)} - y_D'^{(k)} \sin\varphi_0^{(k)} \\ y_D^{(k)} = y_A^{(k)} + x_D'^{(k)} \sin\varphi_0^{(k)} + y_D'^{(k)} \cos\varphi_0^{(k)} \end{cases} \tag{4.1}$$

where:

$$x_D'^{(k)} = x_i'^{(k)} + a' - b'\varphi_i'^{(k)}, \qquad y_D'^{(k)} = y_i'^{(k)} + a'\varphi_i'^{(k)} + b' \tag{4.2}$$

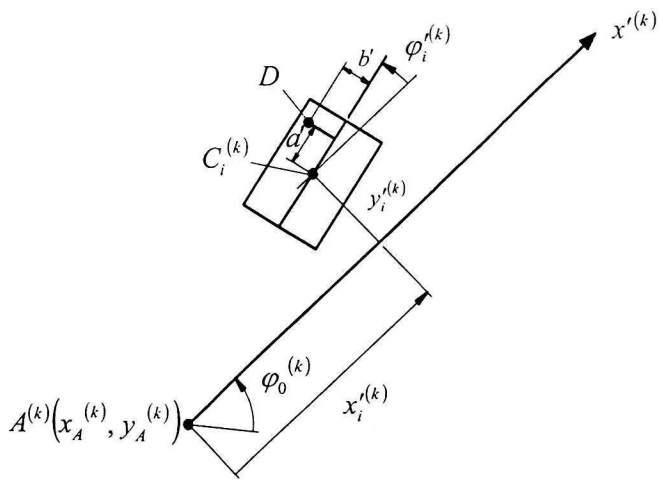

Fig. 4. General coordinates of i[th] rigid element

In particular, the equations (4) allow the coordinates of the centre of mass of the i-th element to be calculated:

$$\begin{cases} x_{Ci}^{(k)} = x_A^{(k)} + x_i'^{(k)} \cos \varphi_0^{(k)} - y_i'^{(k)} \sin \varphi_0^{(k)} \\ y_{Ci}^{(k)} = y_A^{(k)} + x_i'^{(k)} \sin \varphi_0^{(k)} + y_i'^{(k)} \cos \varphi_0^{(k)} \end{cases} \tag{5}$$

The kinetic energy of the i-th element is given by the formula:

$$T_i^{(k)} = \frac{1}{2} m_i^{(k)} \left\{ \left[\dot{x}_{Ci}^{(k)} \right]^2 + \left[\dot{y}_{Ci}^{(k)} \right]^2 \right\} + \frac{1}{2} I_i \left[\dot{\varphi}_0^{(k)} + \dot{\varphi}_i'^{(k)} \right]^2 \tag{6}$$

The equations of motion can be derived from Lagrange's equations. For further discussion, it is convenient to calculate the appropriate operators. In this case, considering the notation (3), they are:

$$\frac{d}{dt} \frac{\partial T_i^{(k)}}{\partial \dot{q}_0^{(k)}} - \frac{\partial T_i^{(k)}}{\partial q_0^{(k)}} = A_{00}^{(k,i)} \ddot{q}_0^{(k)} + A_{0i}^{(k)} \ddot{q}_i^{(k)} + f_0^{(k,i)} \tag{7.1}$$

$$\frac{d}{dt} \frac{\partial T_i^{(k)}}{\partial \dot{q}_i^{(k)}} - \frac{\partial T_i^{(k)}}{\partial q_i^{(k)}} = \left[A_{0i}^{(k)} \right]^T \ddot{q}_0^{(k)} + A_{ii}^{(k)} \ddot{q}_i^{(k)} + f_i^{(k,i)} \tag{7.2}$$

where:

$$A_{00}^{(k,i)} = \begin{bmatrix} m_i^{(k)} & 0 & -m_i^{(k)}[x_i'^{(k)} s_0^{(k)} + y_i'^{(k)} c_0^{(k)}] \\ 0 & m_i^{(k)} & m_i^{(k)}[x_i'^{(k)} c_0^{(k)} - y_i'^{(k)} s_0^{(k)}] \\ -m_i^{(k)}[x_i'^{(k)} s_0^{(k)} + y_i'^{(k)} c_0^{(k)}] & m_i^{(k)}[x_i'^{(k)} c_0^{(k)} - y_i'^{(k)} s_0^{(k)}] & m_i^{(k)}([x_i'^{(k)}]^2 + y_i'^{(k)}]^2) + I_i^{(k)} \end{bmatrix},$$

$$A_{0i}^{(k)} = \begin{bmatrix} m_i^{(k)} c_0^{(k)} & -m_i^{(k)} s_0^{(k)} & 0 \\ m_i^{(k)} s_0^{(k)} & m_i^{(k)} c_0^{(k)} & 0 \\ -m_i^{(k)} y_i'^{(k)} & m_i^{(k)} x_i'^{(k)} & I_i^{(k)} \end{bmatrix}, \qquad A_{ii}^{(k)} = \begin{bmatrix} m_i^{(k)} & 0 & 0 \\ 0 & m_i^{(k)} & 0 \\ 0 & 0 & I_i^{(k)} \end{bmatrix},$$

$$f_0^{(k,i)} = \begin{bmatrix} m_i^{(k)}\left\{-2\dot{\varphi}_0^{(k)}\left[\dot{x}_i'^{(k)} s_0^{(k)} + \dot{y}_i'^{(k)} c_0^{(k)}\right] + \left[\dot{\varphi}_0^{(k)}\right]^2\left(-x_i'^{(k)} c_0^{(k)} + y_i'^{(k)} s_0^{(k)}\right)\right\} \\ m_i^{(k)}\left\{2\dot{\varphi}_0^{(k)}\left[\dot{x}_i'^{(k)} c_0^{(k)} - \dot{y}_i'^{(k)} s_0^{(k)}\right] - \left[\dot{\varphi}_0^{(k)}\right]^2\left(x_i'^{(k)} s_0^{(k)} + y_i'^{(k)} c_0^{(k)}\right)\right\} \\ m_i^{(k)}\left\{2\dot{\varphi}_0^{(k)}\left[x_i'^{(k)} \dot{x}_i'^{(k)} + y_i'^{(k)} \dot{y}_i'^{(k)}\right)\right\} \end{bmatrix},$$

$$f_i^{(k)} = \begin{bmatrix} m_i^{(k)} 2\dot{\varphi}_0^{(k)}\left[-2\dot{y}_i'^{(k)} - x_i'^{(k)} \dot{\varphi}_0^{(k)}\right] \\ m_i^{(k)} 2\dot{\varphi}_0^{(k)}\left[2\dot{x}_i'^{(k)} - y_i'^{(k)} \dot{\varphi}_0^{(k)}\right] \\ 0 \end{bmatrix}, \qquad s_0^{(k)} = \sin \varphi_0^{(k)},\ c_0^{(k)} = \cos \varphi_0^{(k)}.$$

The kinetic energy of the beam equals:

$$T^{(k)} = \sum_{i=0}^{n_k} T_i^{(k)} \tag{8}$$

And thus the Lagrange operator for it is the following:

$$\frac{d}{dt}\frac{\partial T^{(k)}}{\partial \dot{q}^{(k)}} - \frac{\partial T^{(k)}}{\partial q^{(k)}} = A^{(k)}\ddot{q} + f^{(k)} \tag{9}$$

where:

$$A^{(k)} = \begin{bmatrix} \sum_{i=0}^{n_k} A_{00}{}^{(k,i)} & A_{01}{}^{(k)} & \dots & A_{0i}{}^{(k)} & \dots & A_{0n_k}{}^{(k)} \\ \left[A_{01}{}^{(k)}\right]^T & A_{11}{}^{(k)} & \dots & 0 & \dots & 0 \\ \vdots & & & & & \\ \left[A_{0i}{}^{(k)}\right]^T & 0 & \dots & A_{ii}{}^{(k)} & \dots & 0 \\ \vdots & & & & & \\ \left[A_{0n_k}{}^{(k)}\right]^T & 0 & \dots & 0 & \dots & A_{n_k n_k}{}^{(k)} \end{bmatrix}, \qquad f^{(k)} = \begin{bmatrix} \sum_{i=0}^{n_k} f_0{}^{(k,i)} \\ f_1{}^{(k)} \\ \vdots \\ f_i{}^{(k)} \\ \vdots \\ f_{n_k}{}^{(k)} \end{bmatrix}$$

In order to calculate the deformation energy and the function of dissipation of energy for the spring-damping element sde_i (Figure 3) of the analysed subsystem, let it be assumed that the coordinates of that element in the local coordinate systems, connected with rfe $i-1$ and rfe i are:

$$(a_{i,i-1}{}^{(k)}, b_{i,i-1}{}^{(k)}), (a_{i,i}{}^{(k)}, b_{i,i}{}^{(k)}) \tag{10}$$

The deformation energy of the sde_i equals:

$$V_i^{(k)} = \frac{1}{2}c_{i,x}{}^{(k)}\left[x_{i,i}{}'^{(k)} - x'_{i,i-1}{}^{(k)}\right]^2 + \frac{1}{2}c_{i,y}{}^{(k)}\left[y_{i,i}{}'^{(k)} - y'_{i,i-1}{}^{(k)}\right]^2 + \\ + \frac{1}{2}c_{i,\varphi}{}^{(k)}\left[\varphi_i'^{(k)} - \varphi'_{i-1}{}^{(k)} - \varphi'_{i,i-1}{}^{(k)}\right]^2 \tag{11}$$

where: $c_{i,x}{}^{(k)}$ – the coefficient of longitudinal flexibility,
$c_{i,y}{}^{(k)}$ – the coefficient of shearing flexibility,

$c_{i,\varphi}^{(k)}$ – the coefficient of bending flexibility,

$\varphi'^{(k)}_{i,i-1} = \varphi'^{(k)}_i - \varphi'^{(k)}_{i-1}$ – the difference between angles for the unloaded beam,

$x'^{(k)}_{i,i-1}$, $y'^{(k)}_{i,i-1}$, $x'^{(k)}_{i,i}$, $y'^{(k)}_{i,i}$ – can be obtained from (4.2) by substituting a', b' by $a'^{(k)}_{i,i-1}$, $b'^{(k)}_{i,i-1}$ and $a'^{(k)}_{i,i}$, $b'^{(k)}_{i,i}$ respectively.

The function of dissipation energy takes the form:

$$D_i^{(k)} = \frac{1}{2} d_{i,x}^{(k)} \left[\dot{x}'^{(k)}_{i,i} - \dot{x}'^{(k)}_{i,i-1}\right]^2 + \frac{1}{2} d_{i,y}^{(k)} \left[\dot{y}'^{(k)}_{i,i} + \dot{y}'^{(k)}_{i,i-1}\right]^2 + \frac{1}{2} d_{i,\varphi}^{(k)} \left[\dot{\varphi}'^{(k)}_i - \dot{\varphi}'^{(k)}_{i-1}\right]^2 \tag{12}$$

where $d_{i,x}^{(k)}$, $d_{i,y}^{(k)}$, $d_{i,\varphi}^{(k)}$ – are the coefficients of longitudinal, shearing, and bending damping,

$\dot{x}'^{(k)}_{i,i-1}$, $\dot{y}'^{(k)}_{i,i-1}$, $\dot{x}'^{(k)}_{i,i}$, $\dot{y}'^{(k)}_{i,i}$ – can be obtained by differentiation of (4.2)

From the formulae (11) and (12) the following may be derived:

$$\frac{\partial V_i^{(k)}}{\partial q_{i-1}^{(k)}} = K_{i,1}^{(k)} q_{i-1}^{(k)} + K_{i,2}^{(k)} q_i^{(k)} + h_{i,1}^{(k)} \tag{13.1}$$

$$\frac{\partial V_i^{(k)}}{\partial q_i^{(k)}} = K_{i,3}^{(k)} q_{i-1}^{(k)} + K_{i,4}^{(k)} q_i^{(k)} + h_{i,2}^{(k)} \tag{13.2}$$

where: $K_{i,1}^{(k)}$, $K_{i,2}^{(k)}$, $K_{i,3}^{(k)}$, $K_{i,4}^{(k)}$, $h_{i,1}^{(k)}$, $h_{i,2}^{(k)}$ are matrices and vectors with constant coefficients [9].

Likewise:

$$\frac{\partial D_i^{(k)}}{\partial \dot{q}_{i-1}^{(k)}} = L_{i,1}^{(k)} \dot{q}_{i-1}^{(k)} + L_{i,2}^{(k)} \dot{q}_i^{(k)} \tag{14.1}$$

$$\frac{\partial D_i^{(k)}}{\partial \dot{q}_i^{(k)}} = L_{i,3}^{(k)} \dot{q}_{i-1}^{(k)} + L_{i,4}^{(k)} \dot{q}_i^{(k)} \tag{14.2}$$

where: $L_{i,1}^{(k)}$, $L_{i,2}^{(k)} = L_{i,3}^{(k)}$, $L_{i,4}^{(k)}$ matrices with constant coefficients [9].

Since the elastic energy and the dissipation of the whole beam are given by the equations:

$$V^{(k)} = \sum_{i=1}^{n_k} V_i^{(k)}, \tag{15.1}$$

$$D^{(k)} = \sum_{i=1}^{n_k} D_i^{(k)} \tag{15.2}$$

therefore:

$$\frac{\partial V^{(k)}}{\partial q^{(k)}} = C^{(k)} q^{(k)} + h^{(k)} \tag{16.1}$$

$$\frac{\partial D^{(k)}}{\partial \dot{q}^{(k)}} = B^{(k)} \dot{q}^{(k)} \tag{16.2}$$

where: $C^{(k)}$ and $B^{(k)}$ – are symmetric matrices with constant coefficients.

The potential energy of gravity forces is given by the formula:

$$V_g^{(k)} = \sum_{i=0}^{n_k} m_i^{(k)} g\, y_{Ci}^{(k)} \tag{17}$$

where: g – gravity acceleration,
$m_i^{(k)}$ – mass of the i-th element,
$y_{Ci}^{(k)}$ – is given by the equation (5).

After simple transformations it gives:

$$\frac{\partial V_g^{(k)}}{\partial q^{(k)}} = G^{(k)} = \left[G_0^{(k)}\ G_i^{(k)} \ldots G_{n_k}^{(k)} \right]^T \tag{18}$$

where:

$$G_0^{(k)} = g \begin{bmatrix} 0 \\ \sum_{i=0}^{n_k} m_i^{(k)} \\ \sum_{i=0}^{n_k} m_i^{(k)} \left[x_i'^{(k)} c_0^{(k)} - y_i'^{(k)} s_0^{(k)} \right] \end{bmatrix}, \qquad G_i^{(k)} = g \begin{bmatrix} m_i^{(k)} s_0^{(k)} \\ m_i^{(k)} c_0^{(k)} \\ 0 \end{bmatrix} \quad i = 1, \ldots, n_k.$$

3.2. Discretization of hydraulic cylinders

The cylinder is treated as a system of two finite rigid elements, connected by a massless and dimensionless spring - damping element (see Figure 5).

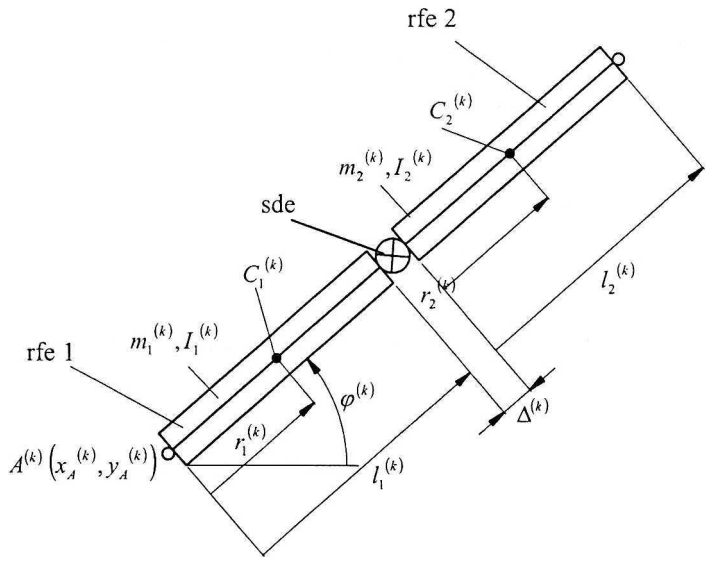

Fig. 5. Discretization of hydraulic cylinder with longitudinal flexibility

With this, the components of the vector of the generalised coordinates of the subsystem are:

$$q^{(k)} = \left[x_A{}^{(k)}\ y_A{}^{(k)}\ \varphi^{(k)}\ \Delta^{(k)}\right]^T \tag{19}$$

where: $x_A{}^{(k)}$, $y_A{}^{(k)}$ – the coordinates of point $A^{(k)}$,
$\varphi^{(k)}$ – the angle of inclination of the cylinder,
$\Delta^{(k)}$ – deformation.

The kinetic energy may be presented as:

$$\begin{aligned} T^{(k)} = {} & \frac{1}{2} m_1{}^{(k)} \left\{ \left[\dot{x}_{C_1}{}^{(k)}\right]^2 + \left[\dot{y}_{C_1}{}^{(k)}\right]^2 \right\} + \frac{1}{2} I_1{}^{(k)} \left[\dot{\varphi}^{(k)}\right]^2 \\ & + \frac{1}{2} m_2{}^{(k)} \left\{ \left[\dot{x}_{C_2}{}^{(k)}\right]^2 + \left[\dot{y}_{C_2}{}^{(k)}\right]^2 \right\} + \frac{1}{2} I_2{}^{(k)} \left[\dot{\varphi}^{(k)}\right]^2 \end{aligned} \tag{20}$$

After transformations we obtained:

$$\frac{d}{dt}\frac{\partial T^{(k)}}{\partial \dot{q}^{(k)}} - \frac{\partial T^{(k)}}{\partial q^{(k)}} = A^{(k)}\ddot{q}^{(k)} + h^{(k)} \tag{21}$$

where: $A^{(k)} = \begin{bmatrix} a_{11} & 0 & a_{13} & a_{14} \\ 0 & a_{22} & a_{23} & a_{24} \\ a_{13} & a_{23} & a_{33} & 0 \\ a_{14} & a_{24} & 0 & a_{44} \end{bmatrix}$.

$$a_{11} = a_{22} = m_1{}^{(k)} + m_2{}^{(k)},\ a_{13} = -\left[m_1{}^{(k)} r_1{}^{(k)} + m_2{}^{(k)}\left(d^{(k)} + \Delta^{(k)}\right)\right] s_\varphi{}^{(k)},\ a_{14} = m_2{}^{(k)} c_\varphi{}^{(k)}$$

$$a_{24} = m_2{}^{(k)} s_\varphi{}^{(k)},\ a_{23} = \left[m_1{}^{(k)} r_1{}^{(k)} + m_2{}^{(k)}\left(d^{(k)} + \Delta^{(k)}\right)\right] c_\varphi{}^{(k)}$$

$$a_{33} = m_1{}^{(k)}\left[r_1{}^{(k)}\right]^2 + I_1{}^{(k)} + m_2{}^{(k)}\left[d^{(k)} + \Delta^{(k)}\right]^2 + I_2{}^{(k)},\ a_{44} = m_2{}^{(k)},$$

$$h^{(k)} = \begin{bmatrix} -\left[m_1{}^{(k)} r_1{}^{(k)} + m_2{}^{(k)}\left(d^{(k)} + \Delta^{(k)}\right)\right]\left[\dot{\varphi}^{(k)}\right]^2 c_\varphi{}^{(k)} - 2m_2{}^{(k)}\dot{\varphi}^{(k)}\dot{\Delta}^{(k)} s_\varphi{}^{(k)} \\ -\left[m_1{}^{(k)} r_1{}^{(k)} + m_2{}^{(k)}\left(d^{(k)} + \Delta^{(k)}\right)\right]\left[\dot{\varphi}^{(k)}\right]^2 s_\varphi{}^{(k)} + 2m_2{}^{(k)}\dot{\varphi}^{(k)}\dot{\Delta}^{(k)} c_\varphi{}^{(k)} \\ 2m_2{}^{(k)}\left(d^{(k)} + \Delta^{(k)}\right)\dot{\Delta}^{(k)}\dot{\varphi}^{(k)} \\ -2m_2{}^{(k)}\left(d^{(k)} + \Delta^{(k)}\right)\dot{\Delta}^{(k)}\dot{\varphi}^{(k)} \end{bmatrix}$$

$$s_\varphi{}^{(k)} = \sin\varphi^{(k)},\ c_\varphi{}^{(k)} = \cos\varphi^{(k)},\ d^{(k)} = l_1{}^{(k)} + r_2{}^{(k)}.$$

The energy of the elastic deformation and the function of dissipation of energy of the spring – damping element may be presented as:

$$V^{(k)} = \frac{1}{2} c_\Delta{}^{(k)}\left[\Delta^{(k)}\right]^2,\quad D^{(k)} = \frac{1}{2} d_\Delta{}^{(k)}\left[\dot{\Delta}^{(k)}\right]^2 \tag{22}$$

where: $c_\Delta{}^{(k)}$, $d_\Delta{}^{(k)}$ – are the coefficients of flexibility and damping of the element.

Thus: $$\frac{\partial V^{(k)}}{\partial q^{(k)}} = C^{(k)} q^{(k)} \tag{23.1}$$

$$\frac{\partial D^{(k)}}{\partial \dot{q}^{(k)}} = B^{(k)} \dot{q}^{(k)} \tag{23.2}$$

where: $C^{(k)} = \begin{bmatrix} 0 & 0 & 0 & 0 \\ 0 & 0 & 0 & 0 \\ 0 & 0 & 0 & 0 \\ 0 & 0 & 0 & c_{\Delta}{}^{(k)} \end{bmatrix}$, $B^{(k)} = \begin{bmatrix} 0 & 0 & 0 & 0 \\ 0 & 0 & 0 & 0 \\ 0 & 0 & 0 & 0 \\ 0 & 0 & 0 & d_{\Delta}{}^{(k)} \end{bmatrix}$.

The potential energy of gravity forces is given by:

$$V_g^{(k)} = m_1{}^{(k)} g\left[y_A{}^{(k)} + r_1{}^{(k)} s_{\varphi}{}^{(k)}\right] + m_2{}^{(k)} g\left[y_A{}^{(k)} + \left(d^{(k)} + \Delta^{(k)}\right) s_{\varphi}{}^{(k)}\right] \tag{24}$$

thus: $$\frac{\partial V_g^{(k)}}{\partial q^{(k)}} = g \begin{bmatrix} 0 \\ m_1{}^{(k)} + m_2{}^{(k)} \\ m_1{}^{(k)} r_1{}^{(k)} + m_2{}^{(k)} \left(d^{(k)} + \Delta^{(k)}\right) c_{\varphi}{}^{(k)} \\ m_2{}^{(k)} s_{\varphi}{}^{(k)} \end{bmatrix} \tag{25}$$

where: $s_{\varphi}{}^{(k)}$, $c_{\varphi}{}^{(k)}$, $d^{(k)}$ – defined in (21).

4. The division of the crane model into subsystems

Figure 6 presents a scheme of a crane model divided into subsystems:

– subsystem {1} modelled by flexible beam, according to the equations from chapter 3.1. The rigid element 0 is the floating unit together with the initial part of the pedestal (rfe 0). In further discussion it has been assumed that the movement of the floating unit is known. It means that the components of the vector:

$$q_0{}^{(1)} = \left[x_A{}^{(1)}\ y_A{}^{(1)}\ \varphi_0{}^{(1)}\right]^T = \left[x_A(t)\ y_A(t)\ \varphi_A(t)\right]^T \tag{26}$$

are not degrees of freedom, but are known functions of time.

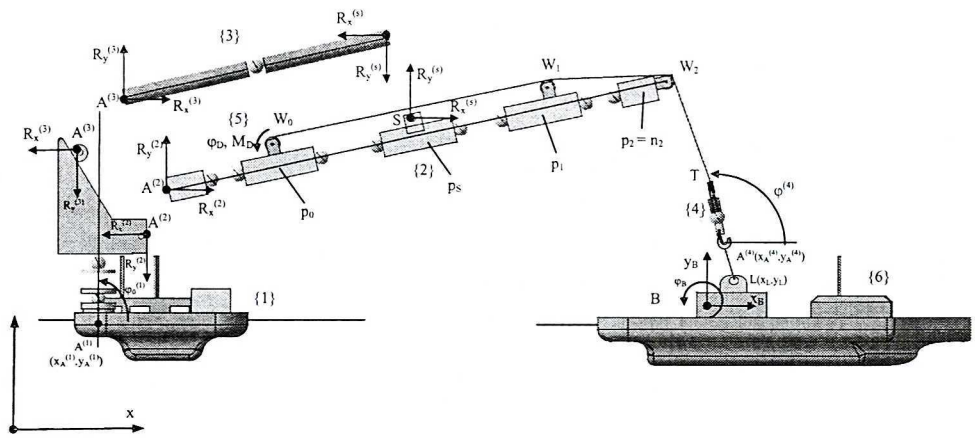

Fig. 6. Subsystems of the considered model

In addition, it is assumed that the element n_1 is not only the final part of the flexible column (pedestal), but also the turning part of the crane.

- subsystem {2}, the jib modelled according to the equations from chapter 3.1. It is assumed that the drum of the hoisting winch is located on the element number p_0, and its coordinates in the local coordinate system are (a_0, b_0). Likewise it is assumed that the sheaves of the rope system are on the elements numbers p_1 and $p_2 = n_2$, and their local coordinates are (a_1, b_1) and (a_2, b_2), respectively. The influence of the turning movement of the sheaves on the system are neglected. When calculating the parameters of elements p_0, p_1, p_2, the mass of the hoisting winch drum and the sheaves must be added to their masses and moments of inertia.
  Hydraulic cylinder {3} is connected with the element p_s, and the local coordinates of the point are (a_s, b_s),
- subsystem {3} is the hydraulic cylinder, modelled according to the equations from chapter 3.2.,
- subsystem {4} is the damper, also modelled according to the equations from chapter 3.2.,
- subsystem {5} is the drum of the hoisting winch. It is assumed that its movement describes the angle of rotation of the drum φ_D,
- subsystem {6} is the load, treated as a lumped mass. Its movement is described by the coordinates of the vector:

$$q_6 = [x_L \; y_L]^T \tag{27}$$

If the load lies on the deck of a floating unit, its coordinates are the known functions of time (coordinates of point B).

The discussion below leads to the formulation of the equations describing the motion of the whole system.

5. The equations of motion of the system

Before formulating the equations of motion of the whole system, the potential energy and the dissipation energy of the rope system should be calculated.

The energy of the elastic deformation of the rope connecting the drum of the hoisting winch and the point T of the damper may be given as:

$$V_l = \frac{1}{2}\delta_l c_l \Delta_l^2 \tag{28}$$

where: $\delta_l = \begin{cases} 1 & \text{if} \quad \Delta_l > 0 \\ 0 & \text{if} \quad \Delta_l \leq 0, \end{cases}$

$$c_l = \frac{E_l F_l}{l_0 - \varphi_D r_D},$$

E_l, F_l – Youngs module and the cross-section area of the rope,
φ_D – the angle of rotation of the hoisting winch,
r_D – radius of winch,
$\Delta_l = l_{W_0W_1} + l_{W_1W_2} + l_{W_2T_2} + \varphi_D r_D - l_0$,
l_0 – the initial length of the rope,

$$l_{W_0W_1} = \left[(x_{W_1} - x_{W_0})^2 + (y_{W_1} - y_{W_0})^2\right]^{\frac{1}{2}},$$

$$l_{W_1W_2} = \left[(x_{W_2} - x_{W_1})^2 + (y_{W_2} - y_{W_1})^2\right]^{\frac{1}{2}},$$

$$l_{W_2T} = \left[(x_T - x_{W_2})^2 + (y_T - y_{W_2})^2\right]^{\frac{1}{2}}.$$

The coordinates of points W_0, W_1, W_2 and T be calculated with the equations:

$$x_{W_j} = x_A^{(2)} + x'_{W_j} c_0^{(2)} - y'_{W_j} s_0^{(2)}, \quad y_{W_j} = y_A^{(2)} + x'_{W_j} s_0^{(2)} + y'_{W_j} c_0^{(2)} \tag{29.1}$$

$$x_T = x_A^{(4)} + \left(l_1^{(4)} + l_2^{(4)} + \Delta^{(k)}\right)\cos\varphi^{(4)}, \quad y_T = y_A^{(4)} + \left(l_1^{(4)} + l_2^{(4)} + \Delta^{(k)}\right)\sin\varphi^{(4)} \tag{29.2}$$

where: $x'_{W_j} = x'^{(2)}_{P_j} + a_j - b_j \varphi'^{(2)}_{P_j}$, $y'_{W_j} = y'^{(2)}_{P_j} + a_j \varphi'^{(2)}_{P_j} + b_j$, $s_0^{(2)}$, $c_0^{(2)}$ – defined in (8);

From (28) we can calculate:

$$\frac{\partial V_l}{\partial q_0^{(2)}}, \frac{\partial V_l}{\partial q_{P_0}^{(2)}}, \frac{\partial V_l}{\partial q_{P_1}^{(2)}}, \frac{\partial V_l}{\partial q_{P_2}^{(2)}}, \frac{\partial V_l}{\partial q^{(4)}}, \frac{\partial V_l}{\partial \varphi_D^{(2)}} \tag{30}$$

The dissipation function of the rope system is given by:

$$D_l = \frac{1}{2} \delta_l d_l \dot{\Delta}_l^2 \tag{31}$$

As in the case of the elastic deformation energy, we can calculate:

$$\frac{\partial D_l}{\partial \dot{q}_0^{(2)}}, \frac{\partial D_l}{\partial \dot{q}_{P_0}^{(2)}}, \frac{\partial D_l}{\partial \dot{q}_{P_1}^{(2)}}, \frac{\partial D_l}{\partial \dot{q}_{P_2}^{(2)}}, \frac{\partial D_l}{\partial \dot{q}^{(4)}}, \frac{\partial D_l}{\partial \dot{\varphi}_D^{(2)}} \tag{32}$$

The fully developed formulae for expressions from (30) and (32) are presented in [22].

The energy of the elastic deformation of the segment $A^{(4)}L$ of the slings and the function of dissipation of energy are given by the formulae:

$$V_L = \frac{1}{2} \delta_L c_L \Delta_L^2, \tag{33.1}$$

$$D_L = \frac{1}{2} \delta_L d_L \dot{\Delta}_L^2 \tag{33.2}$$

where: $\delta_L = \begin{cases} 1 & \text{if} \quad \Delta_l > 0 \\ 0 & \text{if} \quad \Delta_l \leq 0' \end{cases}$

c_L, d_L – are spring and damping coefficients,

$\Delta L = L - L_0$,

$L = \left[\left(x_A^{(4)} - x_L \right)^2 + \left(y_A^{(4)} - y_L \right)^2 \right]^{\frac{1}{2}}$,

L_0 – is the length of the undeformed rope.

Thus, non-zero expressions are only:

$$\frac{\partial V_L}{\partial q^{(4)}} = \delta_L c_L \Delta_L \frac{1}{L}\left\{\left(x_A{}^{(4)} - x_L\right)\frac{\partial x_A{}^{(4)}}{\partial q^{(4)}} + \left(y_A{}^{(4)} - y_L\right)\frac{\partial y_A{}^{(4)}}{\partial q^{(4)}}\right\} \tag{34.1}$$

$$\frac{\partial V_L}{\partial q^{(6)}} = \delta_L c_L \Delta_L \frac{1}{L}\left\{\left(x_A{}^{(4)} - x_L\right)\left(-\frac{\partial x_L}{\partial q^{(6)}}\right) + \left(y_A{}^{(4)} - y_L\right)\left(-\frac{\partial y_L}{\partial q^{(6)}}\right)\right\} \tag{34.2}$$

where: $\dfrac{\partial x_A{}^{(4)}}{\partial q^{(4)}} = \begin{bmatrix}1\\0\\0\\0\end{bmatrix}$; $\dfrac{\partial y_A{}^{(4)}}{\partial q^{(4)}} = \begin{bmatrix}0\\1\\0\\0\end{bmatrix}$; $\dfrac{\partial x_L}{\partial q^{(6)}} = \begin{bmatrix}1\\0\end{bmatrix}$; $\dfrac{\partial y_L}{\partial q^{(6)}} = \begin{bmatrix}0\\1\end{bmatrix}$.

Likewise it may be calculated:

$$\frac{\partial D_L}{\partial \dot{q}^{(4)}}, \qquad \frac{\partial D_L}{\partial \dot{q}^{(6)}}. \tag{35}$$

Considering the above dependencies, the equations of motion of the system may be written as follows:

$$A \cdot \ddot{q} + B \cdot R = F \tag{36}$$

where:

$q = \begin{bmatrix}\bar{q}^{(1)}\\q^{(2)}\\q^{(3)}\\q^{(4)}\\q^{(5)}\\q^{(6)}\end{bmatrix}$ – is a vector of generalised coordinates,

$\bar{q}^{(1)} = \begin{bmatrix}q_1{}^{(1)}\\\vdots\\q_{n_1}{}^{(1)}\end{bmatrix}$, $q_i{}^{(1)}$ – are defined at (3),

$q^{(2)}$ – is defined at (3),

$q^{(3)}, q^{(4)}$ – are defined at (19),

$q^{(5)} = \varphi_D$,
$q^{(6)}$ – is defined at (27);
$R = [R_x^{(2)}\ R_y^{(2)}\ R_x^{(3)}\ R_y^{(3)}\ R_x^{(s)}\ R_y^{(s)}\ R_{Bx}\ R_{By}]^T$ – is the vector of unknown joint forces,
A – is a block matrix with changing coefficients,
B – is a matrix with changing coefficients,
F – is a vector of generalised forces of the potential energy, the dissipation of energy of the spring – damping element, the ropes, and the torque M_D acting on the drum of the hoisting winch.

R_{Bx}, R_{By} are the components of reaction vector R only when the load is in contact with the supply vessel B.
The equations (36) form the system of:

$$m = 3 * n_1 + 3 * (n_2 + 1) + 4 + 4 + 1 + 2 = 3 * (n_1 + n_2) + 14 \tag{37}$$

nonlinear differential equations of the second order with:

$$p = m + 8 \tag{38}$$

unknown values (the components of vectors q and R). Thus, it must be supplemented with the appropriate constraint equations, which in the discussed case are given by:

$$x_A^{(1)} + x'_{A_2} \cos \varphi_0^{(1)} - y'_{A_2} \sin \varphi_0^{(1)} = x_A^{(2)} \tag{39.1}$$

$$y_A^{(1)} + y'_{A_2} \sin \varphi_0^{(1)} + y'_{A_2} \cos \varphi_0^{(1)} = y_A^{(2)} \tag{39.2}$$

$$x_A^{(1)} + x'_{A_3} \cos \varphi_0^{(1)} - y'_{A_3} \sin \varphi_0^{(1)} = x_A^{(3)} \tag{40.1}$$

$$y_A^{(1)} + x'_{A_3} \sin \varphi_0^{(1)} + y'_{A_3} \cos \varphi_0^{(1)} = y_A^{(3)} \tag{40.2}$$

$$x_A^{(3)} + (l_1^{(3)} + l_2^{(3)} + \Delta^{(3)}) \cos \varphi^{(3)} = x_A^{(2)} + x'_s \cos \varphi_0^{(2)} - y'_s \sin \varphi_0^{(2)} \tag{41.1}$$

$$y_A^{(3)} + (l_1^{(3)} + l_2^{(3)} + \Delta^{(3)}) \sin \varphi^{(3)} = y_A^{(2)} + x'_s \sin \varphi_0^{(2)} + y'_s \cos \varphi_0^{(2)} \tag{41.2}$$

$$x_L = x_B(t) \tag{42.1}$$

$$y_L = y_B(t) \tag{42.2}$$

where:

$x'_{A_2} = x'^{(1)}_{n_1} + a_{A_2} - b_{A_2}\varphi'^{(1)}_{n_1}$, $y'_{A_2} = y'^{(1)}_{n_1} + a_{A_2}\varphi'^{(1)}_{n_1} + b_{A_2}$,
a_{A_2}, b_{A_2}– the coordinates of point A_2 in the coordinate system of element n_1,

$x'_{A_3} = x'^{(1)}_{n_1} + a_{A_3} - b_{A_3}\varphi'^{(1)}_{n_1}$, $y'_{A_3} = y'^{(1)}_{n_1} + a_{A_3}\varphi'^{(1)}_{n_1} + b_{A_3}$,
a_{A_3}, b_{A_3}– the coordinates of point A_3 in the coordinate system of element n_1,

$x'_S = x'^{(2)}_{p_s} + a_S - b_S\varphi'^{(2)}_{p_s}$, $y'_S = y'^{(2)}_{p_s} + a_S\varphi'^{(2)}_{p_s} + b_S$,
a_S, b_S– the coordinates of point S in the coordinate system of element p_s in the subsystem 2,

If the load is in the air, the equations (42) are not valid.

The presented model allows the movement of the crane's elements to be analysed for any movement of a unit, on which there is a crane $q_0^{(1)}$ (coordinates $x_{A_{(0)}}^{(1)}$, $y_{A_{(0)}}^{(1)}$, $\varphi_{A_{(0)}}^{(1)}$), and the movement of a unit from which a load is being lifted (coordinates $x_B(t)$, $y_B(t)$, $\varphi_B(t)$). The reaction forces acting in connecting points $A^{(2)}$, $A^{(3)}$, S have also been calculated.

6. Numerical calculations

According to the rigid finite element method presented, primary and secondary division of beam-like links was carried out and a system of rigid elements and connecting spring-damping elements was achieved. Figure 7 presents the primary and secondary discretizations of the jib. The elements with equal length in primary division are presented in Figure 7a. Figure 7b presents the one arbitrarily chosen case, in which strongly non-linear stiffness characteristics of the jib were taken into account.

a)

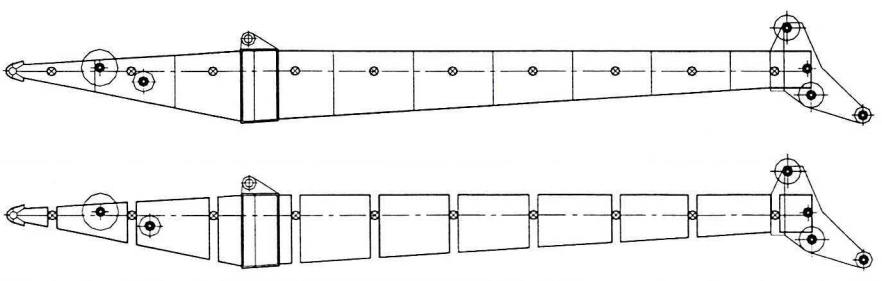

b)

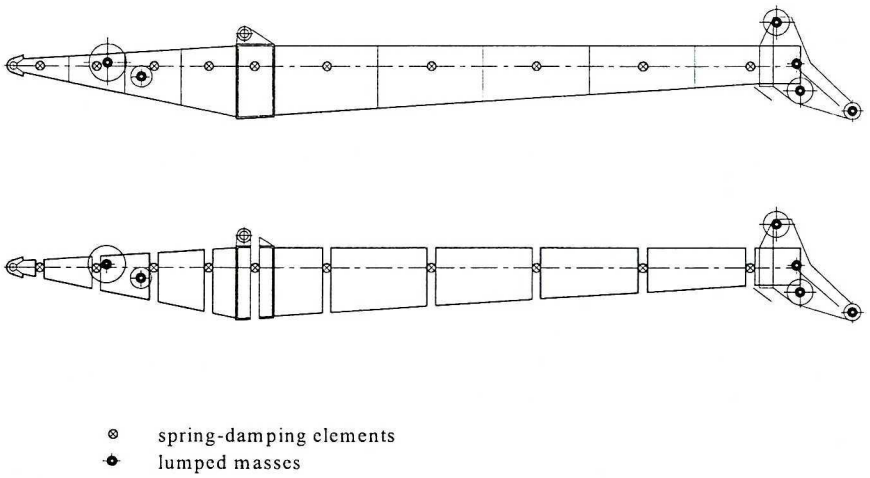

Fig. 7. Primary and secondary division of the jib into rigid and spring – damping elements
a) equal length of elements
b) division takes into account stiffness characteristic of the jib

In both cases, the presented examples concern the case when $n_2 = 10$. Figure 8 presents the inertial moment of cross-section of the jib.

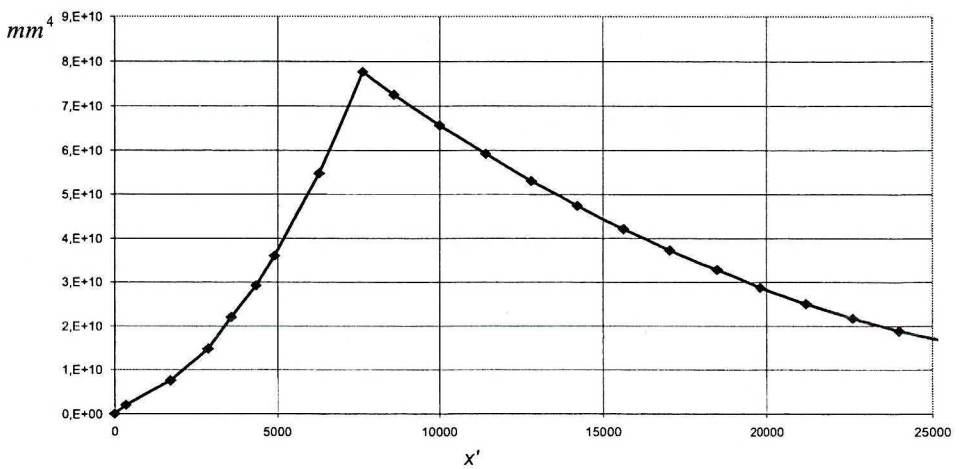

Fig. 8. Inertial moment of jib cross – section

Fig. 9. Support of beam and load in linear vibration and static analysis

The accuracy of the jib discretisation was verified using the calculation scheme shown in Figure 9. The three lowest frequencies and deflections of jib for various number n_2 of elements from Figure 7a are presented in Table 1.

Table 1.
Influence of number of rigid finite elements on frequencies and static deflections of the jib. Point H is defined in Figure 9

n_2	f_1 [Hz]	f_2 [Hz]	f_3 [Hz]	y'_H [mm]	
				$g = 9.81 \frac{m}{s^2}$ $P = 0$	$g = 0$ $P = 2 \cdot 10^5$ N
6	3.731	18.594	25.551	−18.81	−50.42
8	3.763	19.068	25.393	−18.76	−49.46
10	3.731	19.037	28.239	−18.94	−50.49
12	3.763	19.163	27.227	−18.63	−49.58
14	3.700	18.879	27.385	−19.28	−51.28
16	3.763	19.100	27.986	−18.71	−49.94
18	3.763	19.195	27.700	−18.49	−49.29
20	3.731	19.131	28.175	−18.89	−50.21
10	3.731	18.942	27.195	−18.95	−50.44

The last row of Table 1 presents the results obtained for the case from Figure 7b (arbitrary division). For further consideration and calculations, the model from Figure 7b has been accepted and applied.

A special package of programmes was developed based on the presented model. The most part of numerical simulation has been carried out for the crane presented in Figure 1.

The results presented concern the load m_L = 30000 kg and load radius R = 17.7 m.

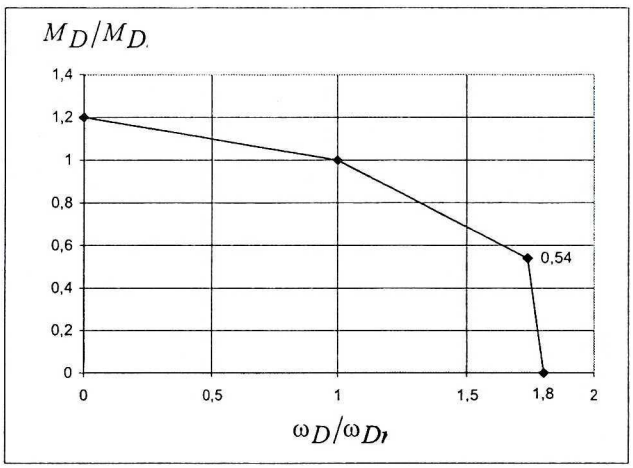

Fig. 10. Hoist drive mechanical characteristics

Hoist drive mechanical characteristics were defined in the following form (see Figure 10):

$$\frac{M_D}{M_{Dnom}} = f\left(\frac{\omega_D}{\omega_{Dnom}}\right) \tag{43}$$

where: M_D is hoist drive torque,
$M_{Dnom} = m_c \cdot g \cdot r_D$ is nominal value of hoist drive torque (static load),
m_c is the working load (mass of the load, hook, shock absorber etc.),
g is gravity acceleration,
r_D is radius of the hoist drum,
ω_D – angular velocity of the hoist drum,
ω_{Dnom} – nominal value of angular velocity of the hoist drum (related to nominal value of hoist velocity of the load).

For the calculations carried out two speeds of reeling rope have been taken into consideration. Their nominal values were equal to 0.45 m/s and 0.8 m/s. The radius of the hoist drum was 0.616 m. It was assumed that the load is lifted from the moving base and motion of the deck of a supply vessel is limited to heave (vertical motion), described as follows:

$$y_B = A \sin(\omega \cdot t + \varphi_0) \tag{44}$$

where: A = 1500 mm is heave amplitude,

$\omega_t = \frac{2\pi}{12}$ 1/s is circular frequency of the heave,

φ_0 is phase angle which defines the start of the lifting operation.

In all cases, it was assumed that the base of crane did not move, so the functions $x_A(t)$, $y_A(t)$, $\varphi_A(t)$ were constant.

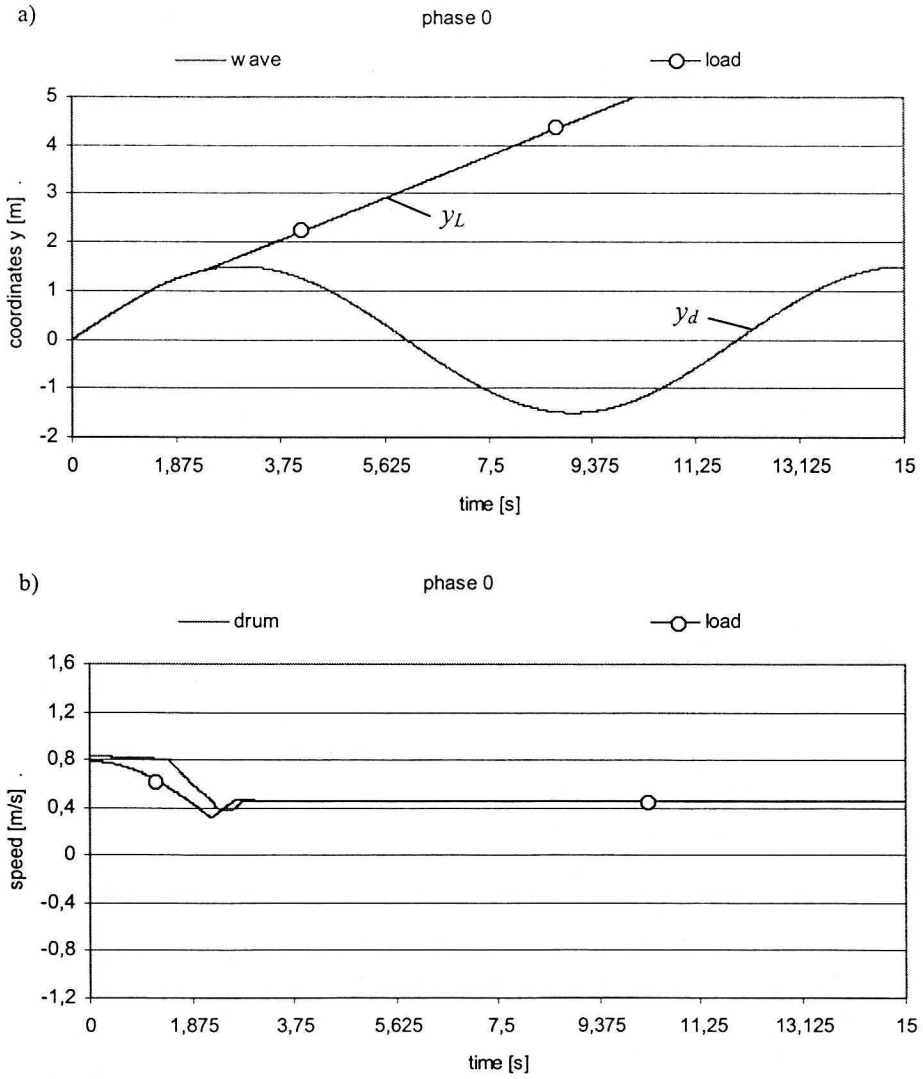

Fig. 11. (a) Vertical displacement y_L and y_d

(b) speeds of the load and the drum for phase angle $\varphi_0 = 0^0$ and nominal load speed 0.46 m/s

The following dynamic coefficient was defined to describe dynamics of the hoisting rope:

$$\eta_L = \frac{F_L}{F_{Lnom}} \tag{45}$$

where: F_L is the force in the hoist rope at the point T (see Figure 6),
$F_{Lnom} = m_c \cdot g$ is a nominal (static) force in the hoist rope.

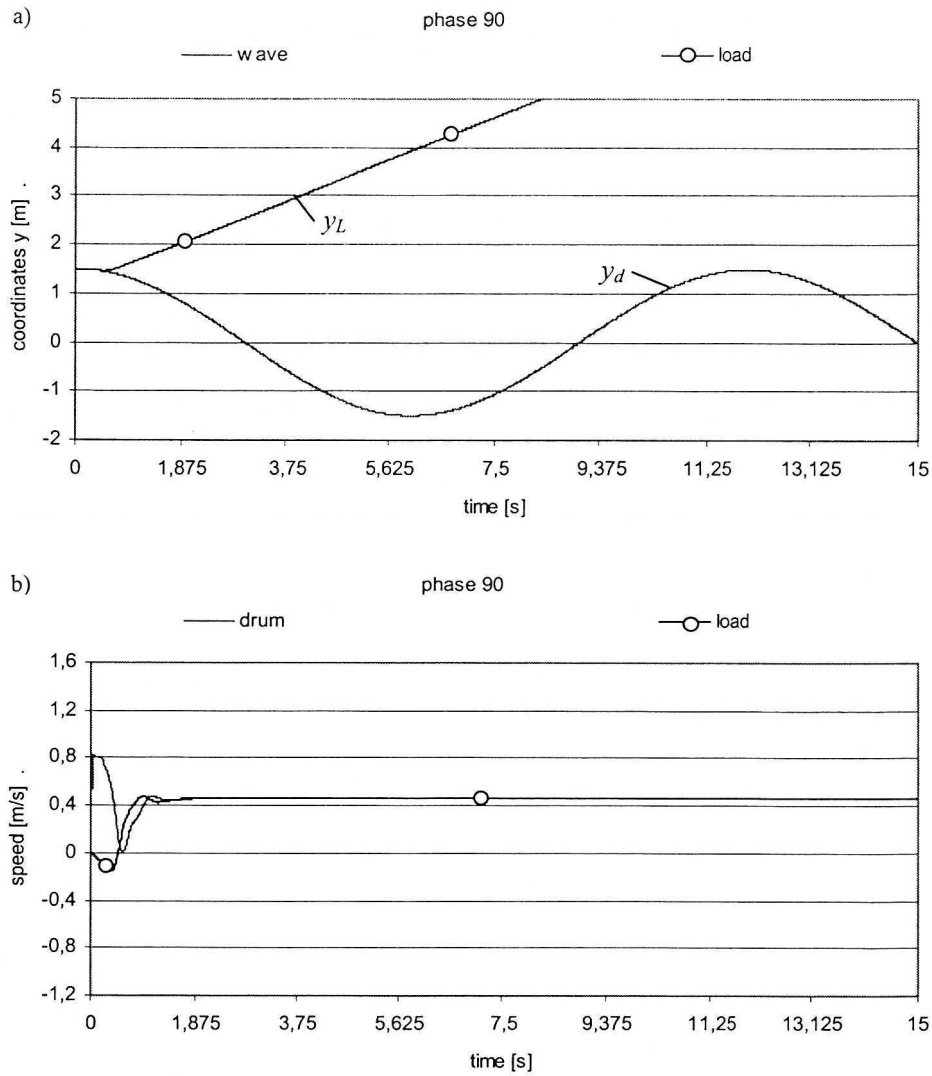

Fig. 12. (a) Vertical displacement y_L and y_d
(b) speeds of the load and the drum for phase angle $\varphi_0 = 90^0$ and nominal load speed 0.46 m/s

Graphs for nominal speed of the load are presented in Figures 11–16. Figures 11–14 show vertical displacements y_L of load and deck y_d of the supply vessel and speeds of the load and the drum for different phases (0°, 90°, 180° and 270°). They demonstrate that the initial phase of lifting the load from the vessel is very important. When the speed of load lifting is not sufficient, the phenomenon of "load tamping" by the deck can occur (Figure 14). On the other hand, this phenomenon does not appear for the same speed but different phase (Figures 11, 12, 13).

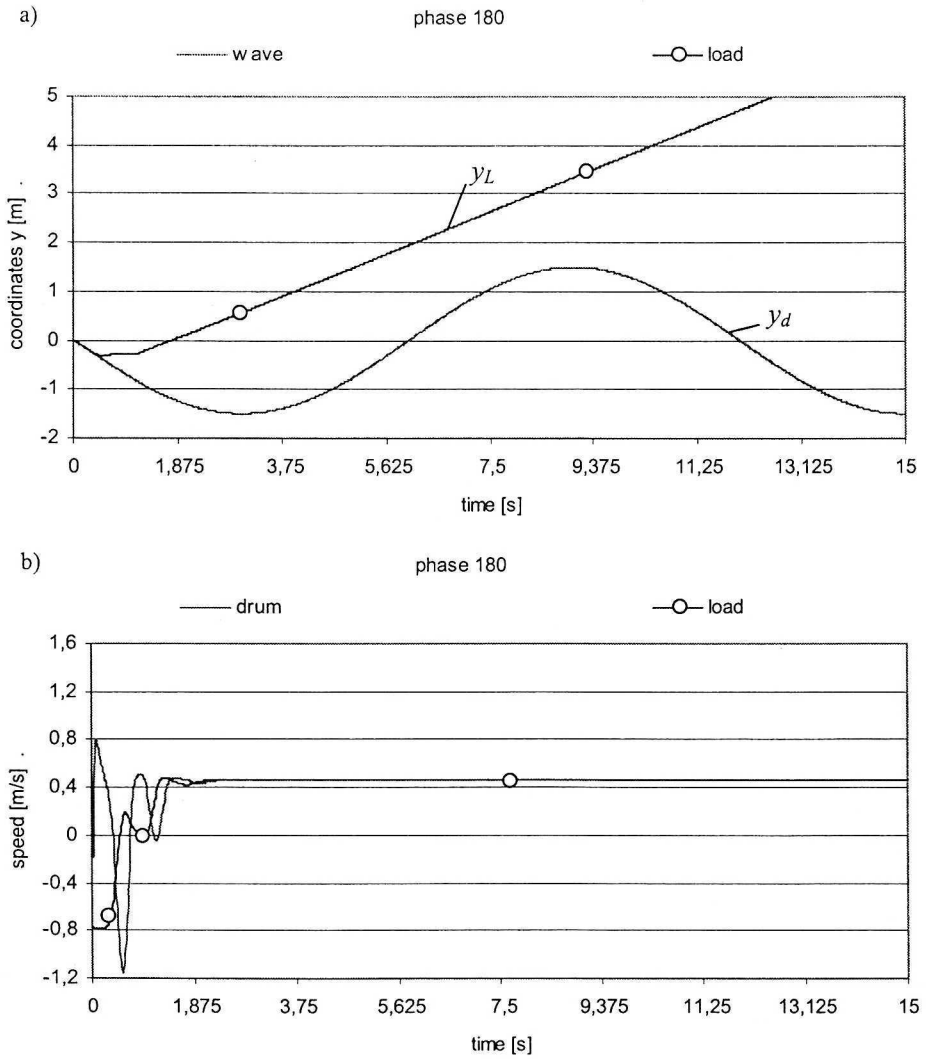

Fig. 13. (a) Vertical displacement y_L and y_d
(b) speeds of the load and the drum for phase angle $\varphi_0 = 180^0$ and nominal load speed 0.46 m/s

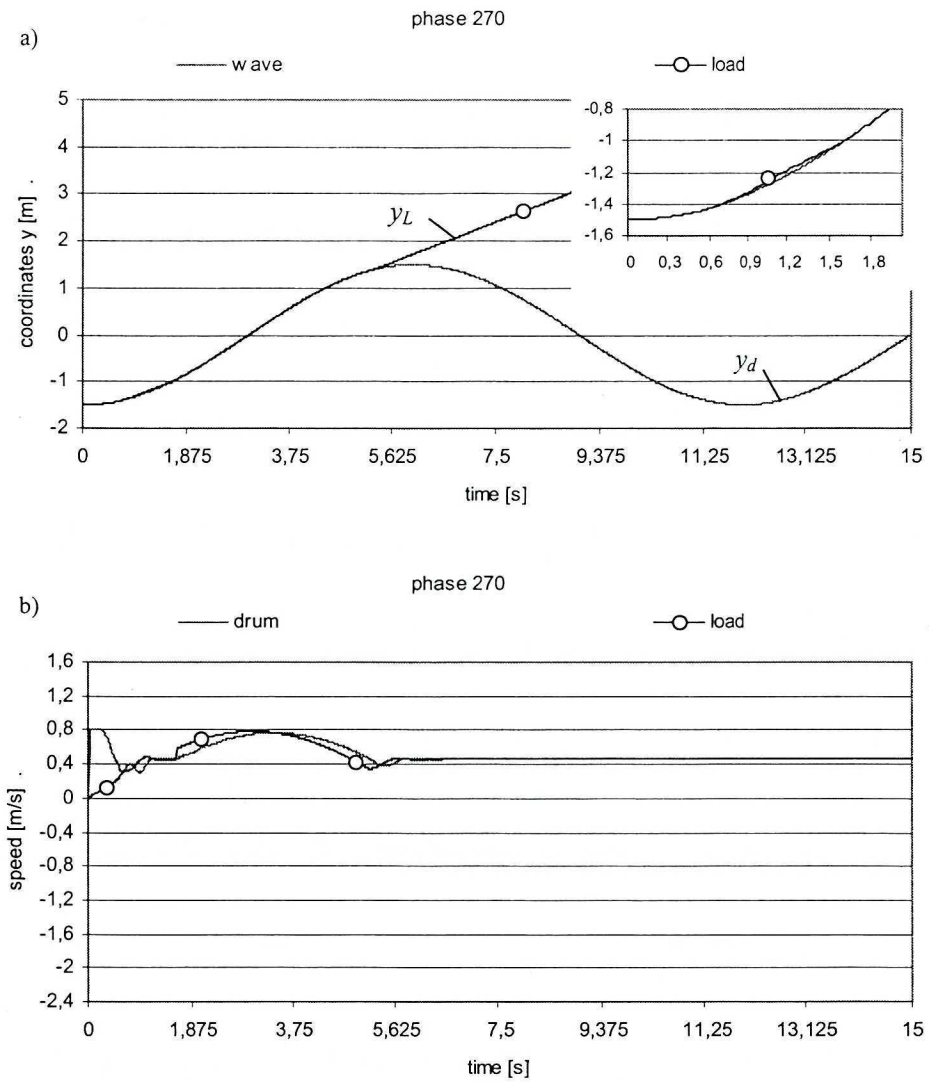

Fig. 14. (a) Vertical displacement y_L and y_d
(b) speeds of the load and the drum for phase angle $\varphi_0 = 270^0$ and nominal load speed 0.46 m/s

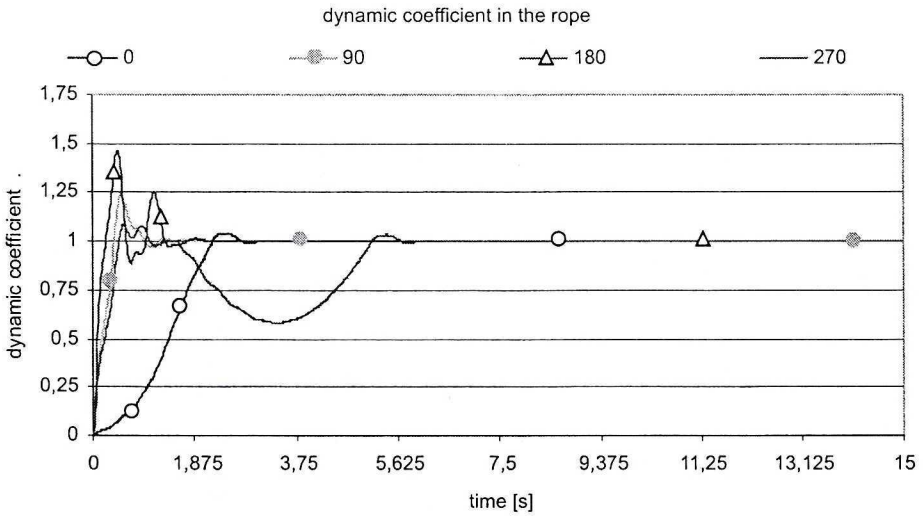

Fig. 15. Hoist rope coefficient η_L course for different phases and nominal load speed 0.46 m/s

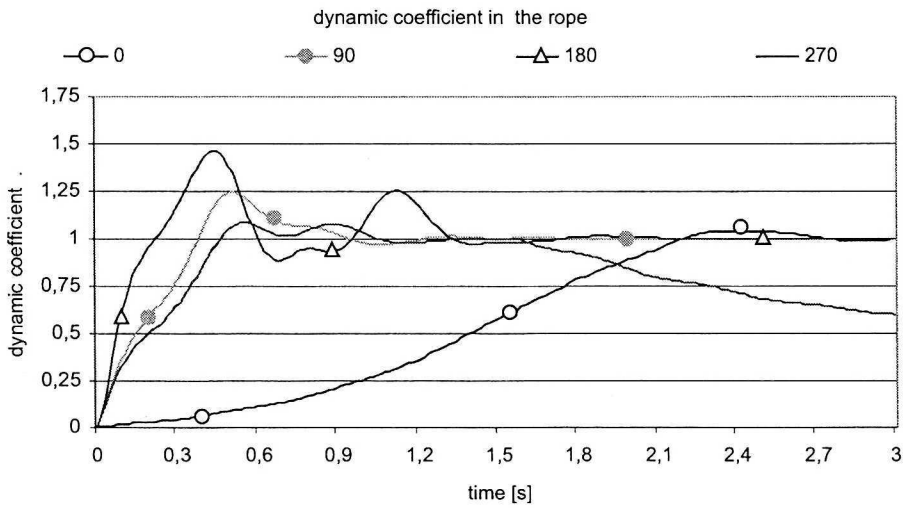

Fig. 16. Hoist rope coefficient η_L course for different phases and nominal load speed 0.46 m/s in first 3 sec

The hoist rope dynamic coefficient η_L for different initial conditions is shown in Figures 15 and 16. Figure 15 presents the time course of this coefficient over 15 sec. The phenomenon of "load tamping" is very well depicted by the curve for 270° phase. Figure 16 shows the time courses over the first 3 sec. By analysing this graph, one can find that for the operating parameters considered lifting the load with 0° phase enables not only motion

without "load tamping", but also ensures the lowest value of dynamic coefficient η_L.

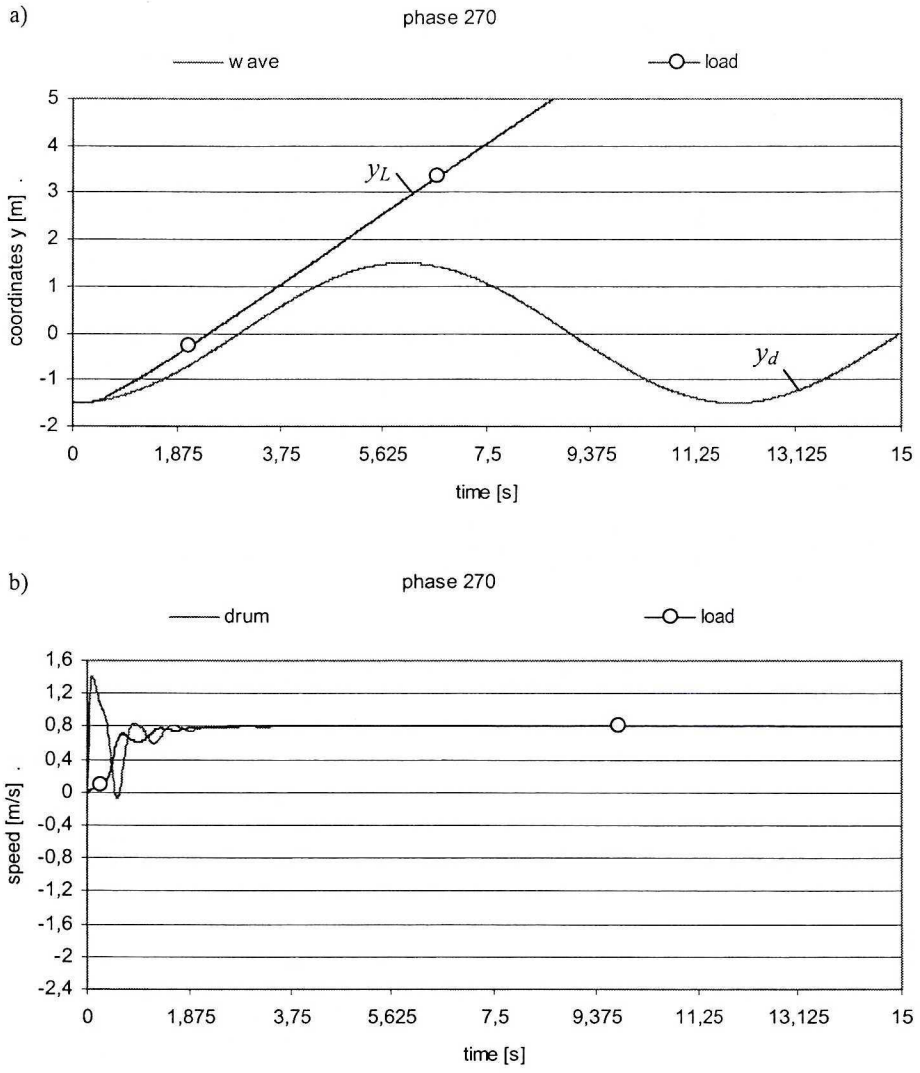

Fig. 17. (a) Vertical displacement y_L and y_d
(b) speeds of the load and the drum for phase angle $\varphi_0 = 270^0$ and nominal load speed 0.8 m/s

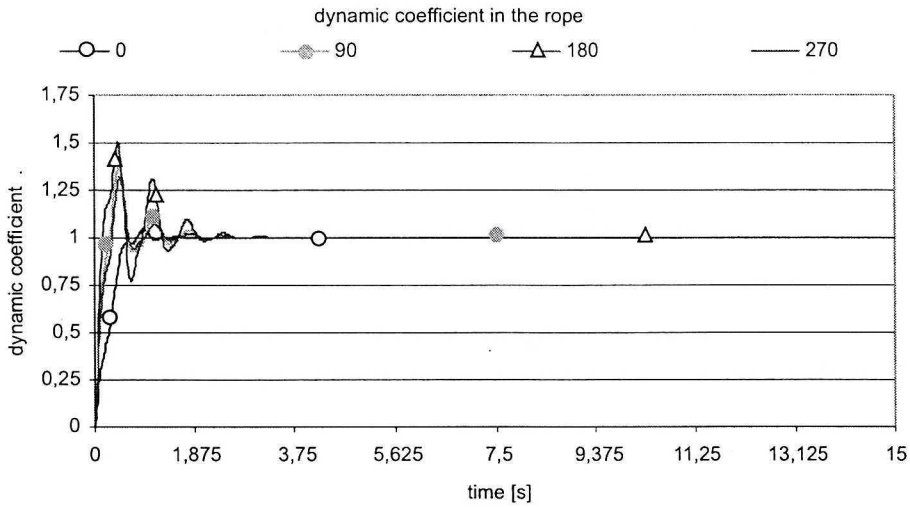

Fig. 18. Hoist rope coefficient η_L course for different phases and nominal load speed 0.8 m/s

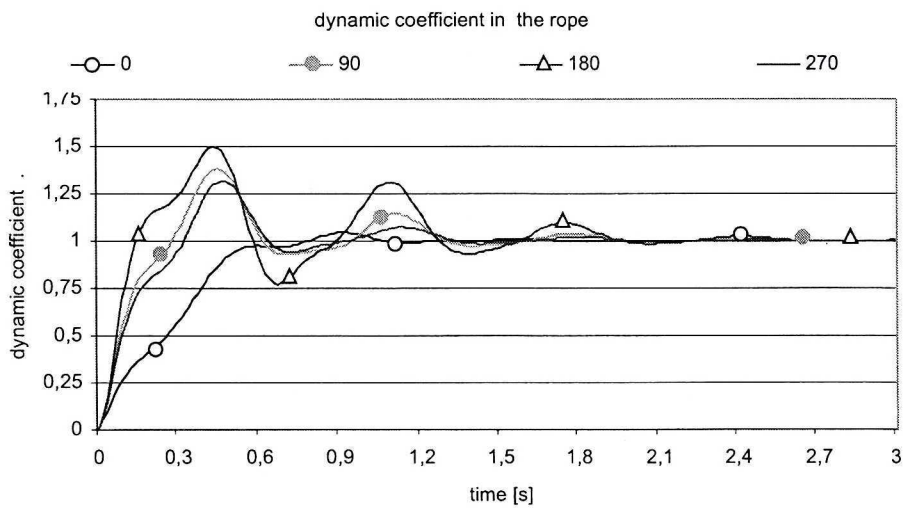

Fig. 19. Hoist rope coefficient η_L course for different phases and nominal load speed 0.8 m/s in first 3 sec

Figures 17–19 have been obtained for the second nominal speed of the load equal to 0.8 m/s. The graph 17 shows vertical displacements of load and deck of the vessel and speeds of the load and the drum for 270° phase. In this phase, for lower nominal speed of the load, "load tamping" occurs. The increase of nominal speed eliminates this phenomenon. Figures 18 and 19 present the time courses of the hoist rope dynamic coefficient η_L over 15 sec and first 3 sec for 0°, 90°, 180° and 270° phases. It should be mentioned that

the results presented in the paper have been obtained for a motionless crane vessel. However, the model and the computer program allow also to take into account the motion of this vessel.

7. Final remarks

In the paper, a dynamic model of the: supply vessel-load-crane-offshore vessel system has been presented. The model takes into account flexibility and damping of the system's elements The rigid finite element method has been applied to discretize the flexible links of the system. Some results of numerical calculations are included. The model elaborated enables dynamic analysis of the system for different operating conditions. The presented model and the developed programmes make it possible to simulate maritime conditions, different drive characteristics and crane parameters. The software can be used during crane design. The model is useful to find out extreme joint and member forces, to optimise parameters of drive units and to establish proper parameters of shock absorbers or dampers.

The nominal crane capacity (safe working load) is normally referred to "zero sea state". The model elaborated can be used for calculation of dynamic load charts – permissible working load for various wave heights. Such a chart or table must be provided for every off-shore crane.

The program could be used also for determination of ultimate load capacity of the crane, sequence of failure and operation risk analysis.

Even if the model is non-linear, the number of degrees of freedom of the system is relatively small as a results of the simple method of discretization, and calculation time for one set of parameters does not exceed a few minutes on a PC.

We hope that the presented model and the newly developed models (e.g. for a spatial system) will be applied as a typical stage of design practice in an off-shore industry.

Manuscript received by Editorial Board, April 03, 2001;
Final version, July 05, 2004.

REFERENCES

[1] Birkeland O.: Knuckle boom combination crane, Materiały 3rd International Offshore Cranes Conference "Offshore Cranes – specification, design, refurbishment, safe operation and maintenance", 27–29 April 1998, Stavanger, Norway.

[2] Balachandran B., Li YY., Fang CC.: A mechanical filter concept for control of non-linear crane-load oscillations, Journal of Sound & Vibration, 228 (3), 1999, pp. 651÷682.

[3] Asfar K., Oqlah F.: A cable manipulation technique for cargo pendulations reduction, 9th Conference on Nonlinear Vibrations, Stability, and Dynamics of Structures, Blacksburg, Virginia, USA, July 28÷31, 2002.
[4] Ellermann K., Kreuzer E., Markiewicz M.: Nonlinear Dynamics of Floating Cranes, Nonlinear Dynamics 27 (2), 2002, pp. 107÷183.
[5] Ellermann K., Kreuzer E., Markiewicz M.: Nonlinear Primary Resonances of a Floating Crane, Meccanica 38, 2003, pp. 5÷18.
[6] Pedrazzi C., Barbieri G.: LARSC: Launch and Recovery Smart cane for naval ROV handling, 13th European ADAMS Users' Conference, Paris, 1998.
[7] Masoud Z. N.: A control system for the reduction of cargo pendulation of ship-mounted cranes, Virginia Polytechnic Institute and State University, Doctoral Thesis, Blacksburg, Virginia, USA, 2000.
[8] Osiński M., Wojciech S.: Some Problems of Dynamic Analysis and Control of an Off-Shore Crane, Materiały 5th International Conference of Cranes and Textile Machines EURO-CRANE'96, Gdańsk, 26–28 February 1996, pp. 114÷125.
[9] Osiński M., Wojciech S.: Dynamic of Hoisting Appliances in Maritime Conditions, Machine Vibration 3, 1994, pp. 76÷84.
[10] Semenov VV.: Kaczka korabla. Sudostrojenie, Leningrad, 1969.
[11] Parker G. G., Groom K., Hurtado J. E., Feddema J., Robinett R. D., Leban F.: Experimental verification of a command shaping boom crane control system, Proceedings of the American Control Conference, San Diego, California, June 1999, pp. 86÷90.
[12] Osiński M., Wojciech S.: Application of Nonlinear Opitmisation Methods to Input Shaping of the Hoist Drive of an Off-Shore Crane, Nonlinear Dynamics 17, 1998, pp. 369÷386.
[13] Fałat P., Wojciech S.: Application of non-linear optimisation methods to stabilise motion of a sea probe, ZN Akademii Techniczno-Humanistycznej w Bielsku-Białej, Zeszyt 6, 2003, pp. 27÷40.
[14] Kruszewski J.: Metoda sztywnych elementów skończonych; Arkady, Warszawa 1975.
[15] Kruszewski J., Sawiak S., Wittbrodt E.: Metoda sztywnych elementów skończonych w dynamice konstrukcji; WNT Warszwa 1999.
[16] Wittbrodt E., Osiński M.: Dynamics of luffing jibs with flexible links, Machine Vibration 2, 1993.
[17] Adamiec I.: Dynamics of a drilling vehicle, Machine Vibration 2, 1993, 223÷228.
[18] Wojciech S.: Dynamics analysis of a manipulator mounted on a car chassis, Machine Vibration 5, 1996, pp. 142÷153.
[19] Wittbrodt E., Wojciech S.: An application of the rigid finite element method to modelling of flexible structures, AIAA Journal of Guidance, Control and Dynamics, Vol. 12, No 4, 1995.
[20] Zienkiewicz O. C.: Metoda elementów skończonych, Arkady, Warszawa 1975.
[21] Osiński M., Wojciech S.: Application of nonlinear optimisation methods to input shaping of the hoist drive of an offshore crane, Nonlinear Dynamics 17, 1998, pp. 369÷386.
[22] Osinski M., Paszkiewicz T., Wojciech S.: Dynamics of lifting appliances on offshore installations, 4th International Offshore Crane Conference, Stavanger, 1999.

Wpływ ruchu statku wywołanego falami regularnymi na dynamikę żurawia typu offshore

Streszczenie

W pracy przestawiono model matematyczny układu: statek dostawczy – ładunek – żuraw – statek przeznaczony do symulacji ruchu oraz analizy dynamicznej układu podczas krytycznych faz

operacji przeładunku ładunku tj. jego podnoszenia lub posadawiania na ruchomym pokładzie jednostki dostawczej. Żurawie pracujące w warunkach offshore poddane są miedzy innymi obciążeniom wynikającym z ruchu zarówno bazy żurawia (statek bazowy, platforma) jak również ruchu jednostki dostawczej wywołanych falowaniem morskim. Na etapie projektowania żurawia niezbędne jest określenie sekwencji zniszczenia poszczególnych elementów (crane failure chart). Opracowany model umożliwia zarówno wyznaczenie maksymalnych sił wewnętrznych i odkształceń elementów układu, jak również symulowanie różnych stanów awaryjnych np. wywołanych nagłą zmianą położenia jednostki względem żurawia. Opracowany model i program obliczeniowy wykorzystywany jest przy projektowaniu nowych i modernizacji istniejących żurawi typu offshore. W artykule zaprezentowano wyniki obliczeń dla przypadku gdy ruch unoszenia statku jest ruchem nurzania.